Formulas for Asymmetric Lead and Lag Compensators

William Messner

Abstract— Lead and lag compensators are commonly used for classical loop shaping and as weighting functions for automated controller synthesis algorithms. The existing formulas for these compensators provide the capability of selecting phase at the frequency of maximum phase lead such that the phase peak or notch is symmetrical on the Bode plot phase chart. This paper develops easy-to-use formulas for lead compensators for choosing the phase at a frequency that is either before, or after the frequency of the maximum phase. For second order compensators, formulas are also provided to specify the degree of asymmetry of the phase peak. Combining these formulas leads to a method for choosing the phase at the frequency of maximum phase for an asymmetric phase peak. An application to a robust controller design problem is shown.

I. INTRODUCTION

Lead and lag compensators are commonly used for classical loop shaping (see e.g. [1], [2]) and as weighting functions for automated controller synthesis algorithms [3]. The existing formulas for these compensators provide the capability of selecting the maximum phase lead and the frequency of maximum phase lead such that the phase peak or notch is symmetrical on the Bode plot phase chart [4].

However it is sometimes desirable in classical loop shaping to provide a specific phase with a lead or lag compensator at a frequency that does not correspond to the frequency of maximum phase lead or phase lag [4]. In other instances, it may be desirable that the phase peak itself not be symmetric. When the phase peak is not symmtric, the associated magnitude response is also altered, and these changes may be desirable for creating weighting functions for automated controller techniques.

This paper is organized as follows. Section II develops easy-to-use formulas for first and second order lead and lag compensators to specify the phase at a compensation frequency that is not the frequency of maximum phase lead or lag. The formulas retain the symmetry of the phase peak or notch on the Bode phase chart. Section III extends formulas for second order lead and lag compensators where the phase peak or notch is *asymmetric* by using different damping ratios for poles and zeros. The phase lead or lag is specified at a compensation frequency that is not generally the frequency of maximum phase or lag. This section also develops a technique to choose both the frequency of maximum phase lead or lag and the phase at that frequency, even though the phase peak is asymmetric. Section IV illustrates the effects of some of the features of these compensators for loop shaping. Section V shows an application of the new asymmetric lead

W. Messner is with Department of Mechanical Engineering, Carnegie Mellon University, 5000 Forbes Avenue, Pittsburgh, Pennsylvania USA
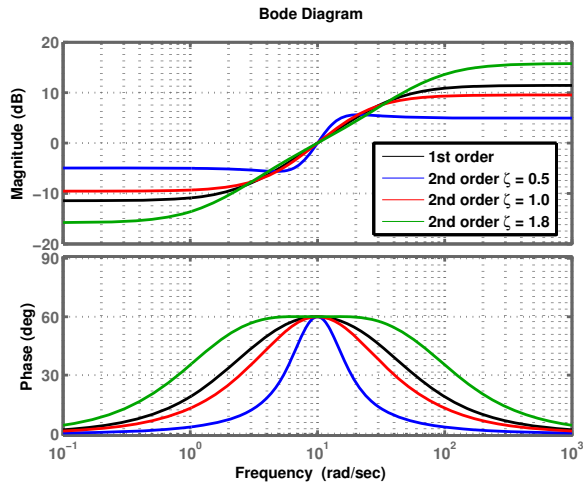bmessner@andrew.cmu.edu

compensator for robust controller design. Section VI contains concluding remarks.

II. SPECIFYING PHASE AT ANY FREQUENCY

A. Lead compensator background

The form of a first order phase lead compensator is

$$C(s) = \frac{s+z}{s+p}. \tag{1}$$

Convenient formulas for specifying the parameters z and p are

$$z = \omega_m \frac{1 - \sin(\phi_m)}{\cos(\phi_m)} \tag{2}$$

$$p = \omega_m \frac{1 + \sin(\phi_m)}{\cos(\phi_m)}, \tag{3}$$

where ω_m is the frequency of maximum phase lead and ϕ_m is the phase at that frequency.

Second order lead compensators have the form

$$C(s) = \frac{s^2 + 2\zeta\omega_z s + \omega_z^2}{s^2 + 2\zeta\omega_p s + \omega_p^2} \tag{4}$$

where

$$
\begin{aligned}
\omega_z &= \omega_m \left(-\zeta\tan(\phi_m) + \sqrt{\zeta^2\tan(\phi_m)^2 + 1} \right) \\
\omega_p &= \omega_m \left(\zeta\tan(\phi_m) + \sqrt{\zeta^2\tan(\phi_m)^2 + 1} \right).
\end{aligned} \tag{5}
$$

ω_m is the frequency of maximum phase, and $2\phi_m$ is the phase at that frequency. The parameter ζ is the damping ratio which can be greater than, equal to, or less than one. Figure 1 shows examples of the a first order compenstor and second order lead compensators with $\omega_m = 10$ and maximum phase lead $90°$. The damping ratios are $\zeta = 0.5$, 1, and 1.8. Note how flat the phase response is for $\zeta = 0.8$.

B. Phase contributions of second order zeros and poles

The phase contribution of the zeros of (4) at $s = j\omega_m$ is given by

$$\phi_z \overset{\triangle}{=} \arg\left(-\omega_m^2 + 2j\zeta\omega_z\omega_m + \omega_z^2 \right). \tag{6}$$

Fig. 1. First and second lead compensators with peak phase lead of 90° at $\omega_m = 10$. Damping ratios for second order compenstors $\zeta = 0.5$, 1, and 1.8.

By taking the tangent of this angle we can determine the value phase contribution of the zero.

$$
\begin{aligned}
\tan(\phi_z) &= \frac{2\zeta\omega_z\omega_m}{\omega_z^2 - \omega_m^2} \\
&= \frac{2\zeta\omega_m^2(-\zeta\tan(\phi_m) + \sqrt{\zeta^2\tan(\phi_m)^2 + 1})}{\omega_m^2(-\zeta\tan(\phi_m) + \sqrt{\zeta^2\tan(\phi_m)^2 + 1})^2 - \omega_m^2} \\
&= \frac{2\zeta(-\zeta\tan(\phi_m) + \sqrt{\zeta^2\tan(\phi_m)^2 + 1})}{2\zeta^2\tan(\phi_m)^2 + 2\zeta\tan(\phi_m)\sqrt{\zeta^2\tan(\phi_m)^2 + 1}} \\
&= \frac{-1}{\tan(\phi_m)} = \tan(\phi_m + 90°). \quad (7)
\end{aligned}
$$

Thus the contribution of the zeros at $s = j\omega_m$ is $\phi_m + 90°$. A similar derivation shows that that the phase contribution of the poles at $s = j\omega_m$ is

$$
\phi_p \overset{\triangle}{=} -\arg\left(-\omega_m^2 + 2j\zeta\omega_p\omega_m + \omega_p^2\right) = \phi_m - 90°. \quad (8)
$$

C. Phase contributions of first order zeros and poles

In the special case where $\zeta = 1$, the zeros and the poles are real. The compensator (4) has the form of a double lead compensator.

$$
C(s) = \frac{s^2 + 2\zeta\omega_z s + \omega_z^2}{s^2 + 2\zeta\omega_p s + \omega_p^2} = \frac{(s+z)^2}{(s+p)^2} \quad (9)
$$

where z and p are given by (2) and (3) respectively.

Each real zero contributes half of the total contribution of the zeros, and each pole contributes half of the total contribution for the poles. Thus the contribution of the zero of a *single* lead compensator is $\frac{\phi_m}{2} + 45°$, and contribution of the pole is $\frac{\phi_m}{2} - 45°$.

D. Formulas for first order compensators

The contributions of the zero and pole of a first order lead compensator can be used to specify the phase contribution

away from the phase peak using the following variations of (2) and (3).

$$
z = \omega_c \frac{1 - \sin(\phi_c - \delta)}{\cos(\phi_c - \delta)} \quad (10)
$$

and

$$
p = \omega_c \frac{1 + \sin(\phi_c + \delta)}{\cos(\phi_c + \delta)}, \quad (11)
$$

where ω_c is the compensation frequency, and $|\delta| < 90° - |\phi_c|$. At $s = j\omega_c$ the contribution of the zero will be $\frac{\phi_c - \delta}{2} + 45°$, and the contribution of the pole will be $\frac{\phi_c + \delta}{2} - 45°$. Thus, the total contribution to the phase at $s = j\omega_c$ will be ϕ_c.

Note that the frequency of maximum phase lead (lag) ω_m relates to ω_c as

$$
\omega_m \begin{cases} > \omega_c & for \ \delta > 0 \\ < \omega_c & for \ \delta < 0. \end{cases} \quad (12)
$$

Figure 2 shows an example where $\omega_c = 10$, $\phi_c = 60°$, and $\delta = 20°$, and the gain has been normalized to 1 at ω_c.

E. Formulas for second order compensators

The same trick applied for first order compensators can be applied to second order compensators as well. Define

$$
\begin{aligned}
\omega_z &= \omega_c\left(-\zeta\tan(\phi_c - \delta) + \sqrt{\zeta^2\tan(\phi_c - \delta)^2 + 1}\right) \\
\omega_p &= \omega_c\left(\zeta\tan(\phi_c + \delta) + \sqrt{\zeta^2\tan(\phi_c - \delta)^2 + 1}\right) \quad (13)
\end{aligned}
$$

where $|\delta| < 90° - |\phi_c|$. For the compensator of the form (4) the phase contribution of the zeros and poles at $s = j\omega_c$ will be $\phi_c - \delta + 90°$ and $\phi_c + \delta - 90°$ respectively, and the total phase contribution will be $2\phi_c$.

Figure 2 shows examples of the second order lead compensators with $\omega_c = 10$, $2\phi_c = 90°$, and $\zeta = 0.5$, 1, 1.8, and $\delta = 30°$. The gain at $\omega_c = 10$ has been normalized to unity.
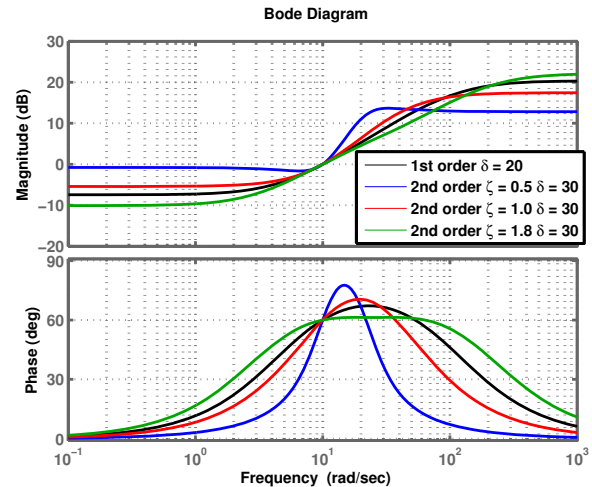

Fig. 2. First and second order lead compensators providing 60° at $\omega_c = 10$, which is not the frequency of the maximum phase.

III. ASYMMETRIC PHASE COMPENSATORS

A. Distinct Damping Ratios

Equations (7) and (8) imply that the phase contribution of the zeros and the poles at $s = j\omega_c$ depend only on the the value of ϕ_c and not on the damping ratio ζ. Therefore, one can choose different damping ratios, $\zeta_z \neq \zeta_p$, for the numerator and denominator of

$$C(s) = \frac{s^2 + 2\zeta_z\omega_z s + \omega_z^2}{s^2 + 2\zeta_p\omega_p s + \omega_p^2} \qquad (14)$$

where

$$\begin{aligned}
\omega_z &= \omega_c\left(-\zeta_z\tan(\phi_c - \delta) + \sqrt{\zeta_z^2\tan(\phi_c - \delta)^2 + 1}\right) \\
\omega_p &= \omega_c\left(\zeta_p\tan(\phi_c + \delta) + \sqrt{\zeta_p^2\tan(\phi_c - \delta)^2 + 1}\right) .(15)
\end{aligned}$$

The phase contribution of the zeros at $s = j\omega_c$ does not depend on ζ_z, and therefore will be $\phi_c - \delta + 90°$. Likewise, the phase contribution of the poles at $s = j\omega_c$ will be $\phi_c + \delta - 90°$, and the total contribution will be $2\phi_c$. However, the phase plot will no longer be symmetric about the frequency of maximum phase ω_m. Also, when $\delta = 0$, the relation between the ω_c and the maximum phase will be

$$\omega_m \begin{cases} > \omega_c & for \ \zeta_p > \zeta_z \\ < \omega_c & for \ \zeta_p < \zeta_z. \end{cases} \qquad (16)$$

Figure 3 shows a comparison of a first order lead compensator, a double lead compensator, and two where the damping ratio of the poles is different from the zeros. All provide 60° of phase at $\omega_c = 10$ with unity gain at ω_c. The peaks of the two compensators with unequal damping ratios are not symmetric. Also note that how the asymmetric lead compensator with $\zeta_z = 0.7$, $\zeta_p = 5.0$, and $\delta = 44.4°$ exhibits both lag as well as lead characteristics.

B. Asymmetric compensators with peak at ω_c

It is possible to manipulate the frequency of maximum phase ω_m for a given ζ_z and ζ_p by choosing δ. In particular it is possible to choose δ such that $\omega_m = \omega_c$. Selection of the appropriate δ can be done manually or by automatically by a bisection search as follows.

1) Choose $\phi_c > 0$, ω_c, ζ_z, and ζ_p and a tolerance $\varepsilon > 0$.
2) Initialize $\delta_{step} = (90° - |\phi_c|)$ and $\delta = 0$
3) Let $\delta_{step} = \frac{1}{2}\delta_{step}$
4) Determine frequency of maximum phase lead ω_m for the compensator defined by (15) for the given δ.
5) If $\omega_m > \omega_c + \varepsilon$, let $\delta = \delta - \delta_{step}$ and go to Step 3.
6) If $\omega_m < \omega_c - \varepsilon$, let $\delta = \delta + \delta_{step}$ and go to Step 3.
7) If $\omega_c - \varepsilon < \omega_m < \omega_c + \varepsilon$, stop.

The δ of the asymmetric lead with $\delta = 44.4°$ in Figure 3 was chosen to make $\omega_m = \omega_c$ by this method. The algorithm converged to $|\omega_m - \omega_c| < \varepsilon = 0.0001°$ in less than 10 steps.

IV. LOOP SHAPING EFFECTS

To providea a simple illustration of the potential utility of these new compensator structures, they are applied to proportional-lead compensation of a double integrator with a design specification of 60° of phase margin at $\omega = 10$. The phase margin of 60° ensures that the open-loop 0 dB crossover, sensitivity function crossover, and the complementary sensitivity function crossover all occur at the same frequency.

Figure 4 shows five open-loop frequency responses of the compensated double integrator with different lead compensators. The asymmetric lead compensator exhibits the highest low frequency gain and good high frequency gain drop-off, but has relatively shallow slope near the 0 dB crossover. The standard first order lead exhibits the smallest low frequency gain, but has good high frequency gain drop-off.
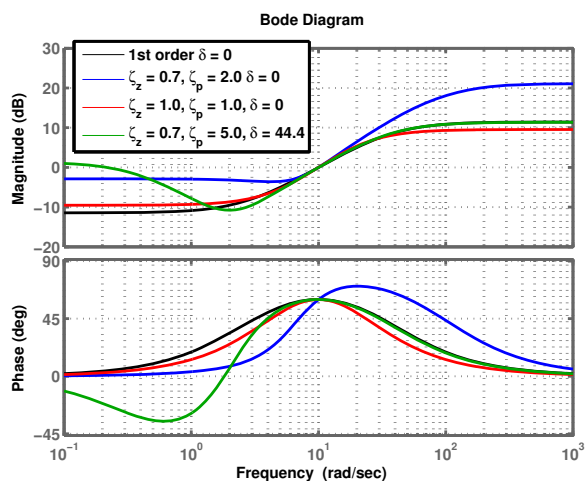

Fig. 3. First order lead compensator, double lead compensator, and two asymmetric lead compensators providing 60° of phase at $\omega_c = 10$ with unity gain at ω_c. The δ of the asymmetric lead with $\delta = 44.4°$ was chosen to make $\omega_m = \omega_c$ for that compensator.
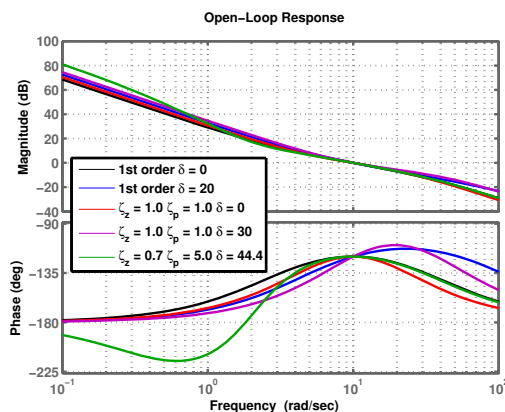

Fig. 4. Open-loop frequency response of the double integrator with five different lead compensators.

Figures 5 and 6 show the five corresponding sensitivity function magnitude responses. The asymmetric lead compensator with $\delta = 44.4°$ exhibits the best disturbance rejection at the low frequencies by at least 6 dB, but the lowest mid
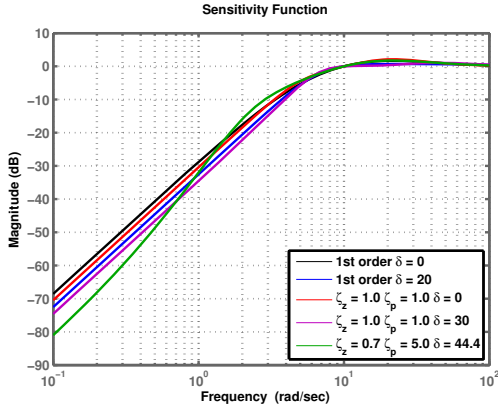
Fig. 5. Magnitude response of the sensitivity functions.

frequency rejection. The second order lead with $\zeta_z = \zeta_p = 1$ and $\delta = 30$ has the best mid frequency disturbance rejection and extremely low peaking above the 0 dB crossover.
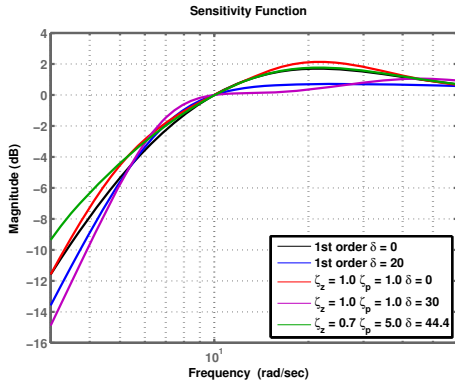

Fig. 6. Close-up of magnitude response of the sensitivity functions.

V. APPLICATION TO ROBUST CONTROL DESIGN

The Robust Bode plot (RBode plot) was developed in [6] and [7]. It allows enables controllers to be designed for robust performance even when the weighting functions are not the magnitude responses of realizable transfer functions.

For this example we consider robust controller design for a nominal system represented with transfer function

$$P_{nom}(s) = \frac{7 \times 10^4}{s^2 + 593s + 4.4 \times 10^4}. \tag{17}$$

Figure 7 shows the frequency response of the nominal model

The actual model is represented by the multiplicative uncertainty

$$P(s) = P_{nom}(s)(1 + \Delta(s)). \tag{18}$$

The function $\Delta(s)$ is a stable transfer function bounded by the uncertainty weighting $W_u(\omega) \geq 0$.

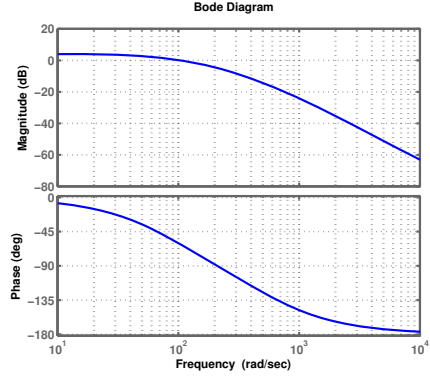$$|\Delta(j\omega)| \leq W_u(\omega) \tag{19}$$

Fig. 7. Frequency response of the nominal model of the plant.

for all $\omega \geq 0$. Figure 8 shows $W_u(\omega)$. The uncertainty is low below 1000 rad/sec. The large peak between 3000 and 3500 rad/sec is the frequency range in which a lightly damped resonance can occur. Note that $W_u(\omega)$ is not the magnitude response of a realizable transfer function in this case. Figure 7 shows the frequency response of the nominal model
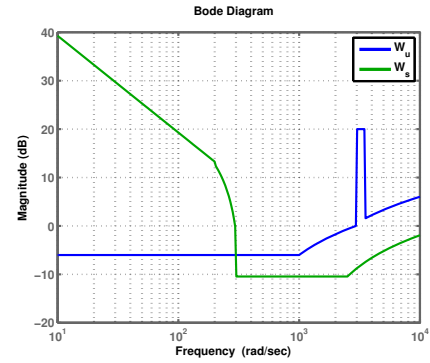

Fig. 8. The uncertainty weighting function $W_u(\omega)$ and the sensitivity weighting function $W_s(\omega)$.

The performance objective is that

$$S(s) \triangleq \frac{1}{1 + P(s)C(s)} \tag{20}$$

satisfies

$$|S(j\omega)| \leq W_s^{-1}(\omega) \tag{21}$$

for all ω. Figure 8 shows the sensitivity weighting function as a function of frequency, which is clearly not the magnitude of a realizable transfer function.

A necessary and sufficient condition for robust performance [8] is that

$$|W_s(\omega)S_{nom}(j\omega)| + |W_u(\omega)T_{nom}(j\omega)| < 1 \tag{22}$$

for all ω where $T(s) \triangleq \frac{P(s)C(s)}{1 + P(s)C(s)}$. The RBode plot translates this criterion into allowable and forbidden regions on the open-loop Bode plot. If there are any intersections between the open-loop response and the forbidden regions, then the

robust performance criterion is not satisfied. Figure 9 shows the RBode plot for the system with no compensation. Clearly robust performance is not achieved
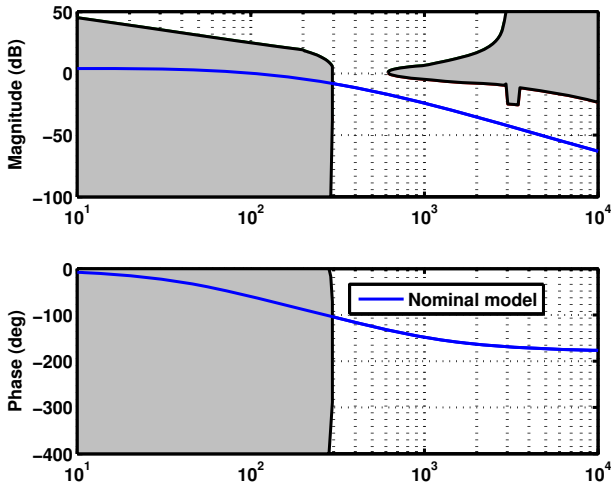

Fig. 9. RBode plot for open-loop response with no compenation.

The procedure for designing a robust controller with the RBode plot is to address low frequency intersections first. Design proceeds by iteratively modifying the compensators as intersections are eliminated at the lower frequencies and new ones appear at higher frequencies. Intersections can either be addressed on the magnitude chart or on the phase chart. If an intersection is eliminated on one chart, it is automatically eliminated on the other.

Figure 10 shows the RBode plot afer applying the PI compensator $C_{PI} = 16\frac{s+100}{s}$. The low frequency intersections are eliminated, but two more appear at higher frequencies.
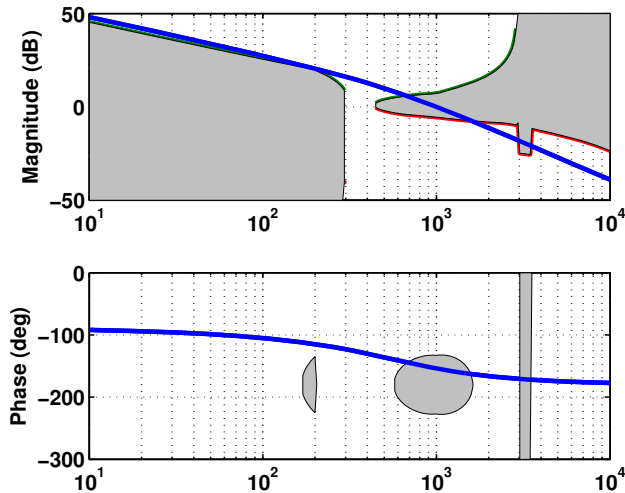

Fig. 10. RBode plot for open-loop response with PI compenation.

The next iteration attempts to address intersections be-

tween 900 and 1600 rad/sec by simultaneously lifting the phase over forbidden region on the magnitude plot using lead compensation and tucking the magnitude response under the forbidden region on the magnitude response. The phase must rise about 30 degrees to avoid the forbidden region on the phase plot.

Figure 11 shows the frequency response of an asymmetric lead compenator where $\omega_c = 1800$ rad/sec, $\phi_c = 40°$, $\zeta_z = 0.7$, $\zeta_p = 3$, and $\delta = -49°$. Note that the compensator exhibits lag properties at lower frequencies even though $\phi_c > 0$ at ω_c. Alternatively, the compensator with these parameters has the form of an asymmetric notch, where the phase is not zero at the frequency of the notch.
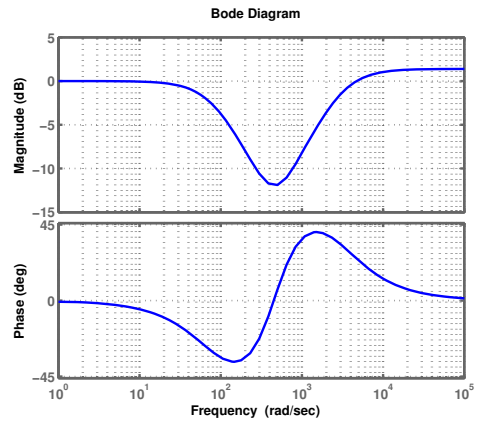

Fig. 11. Frequency response for asymmetric lead compenator where $\omega_c = 1800$ rad/sec, $\phi_c = 40°$, $\zeta_z = 0.7$, $\zeta_p = 3$, and $\delta = -49°$.

Figure 12 shows the RBode plot with PI compensation, asymmetric lead compensation, and gain adjustment. Only an intersection between 3000 and 3500 rad/sec.
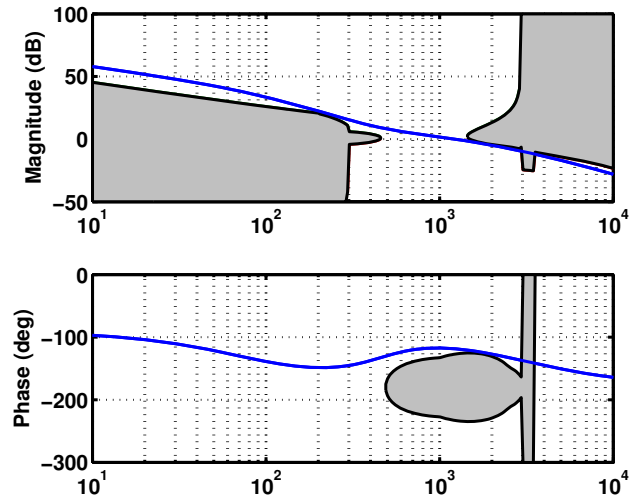

Fig. 12. RBode plot for the open loop with PI and asymmetric lead compensation.

For the final intersection, we apply a phase adjustable notch [9]. Figure 13 shows the frequency response of a phase adjustable with $\omega_{notch} = 3233\ rad/sec$, a notch depth of 120 dB, $\phi_{notch} = 45°$, and $\zeta_p = 0.26$ for the damping ratio of the poles of the compensator.

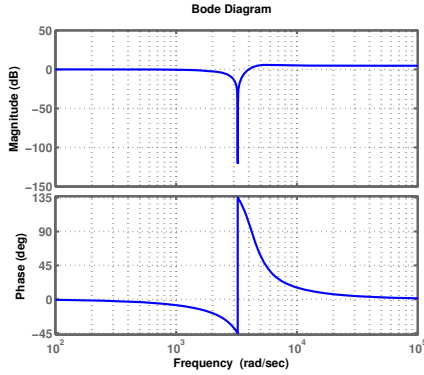

Fig. 13. Frequency response of a phase adjustable notch with $\omega_{notch} = 3233\ rad/sec$, a notch depth of 120 dB, $\phi_{notch} = 45°$, and $\zeta_p = 0.26$.

Figure 14 shows the RBode plot after the application of the phase adjustable notch. All intersections with forbidden regions have been eliminated. The final compensator is

$$C(s) = 85\frac{(s+100)(s^2+645.6s+2.127\times 10^5)}{s(s+2891)} \times$$
$$\frac{(s^2+0.001891s+1.045\times 10^7)}{(s+91.46)(s^2+2280s+\times 10^7)}, \quad (23)$$

which is only 5th order. Figure 15 shows the plot of $|W_s(\omega)S(j\omega)| + |W_u(\omega)T(j\omega)|$ confirming that robust performance is achieved.
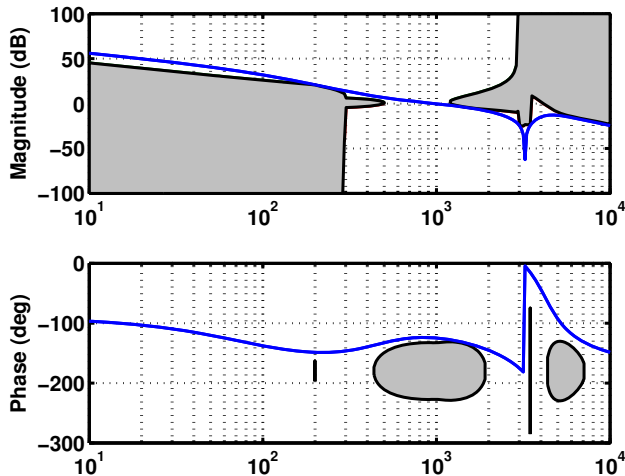

Fig. 14. RBode plot after phase adjustable notch compensation. All intersection have been eliminated.
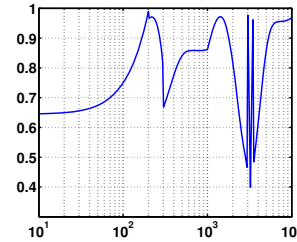

Fig. 15. Plot $|W_s(\omega)S(j\omega)| + |W_u(\omega)T(j\omega)|$ confirming robust performance has been achieved.

VI. CONCLUSIONS AND FUTURE WORK

This paper developed new formulas for lead and lag compensators that allow the design engineer to specify the phase lead or lag at frequencies other than the frequency of maximum phase lead or lag. Formulas for lead and lag compensators where the phase peak or phase notch is not symmetric were also presented. An algorithm was presented for ensuring that the maximum phase lead or lag occurs at the specified compensation frequency, even when the phase peak is not symmetric. A proportional lead compensator design provided a simple illustration of some of the properties of these compensators. The paper also showed an application to a robust performance controller design problem employing the RBode plot. It is believed that these formulas will be very useful to practioners of who use loop shaping.

REFERENCES

[1] G.F. Franklin, J.D. Powell, and A. Emani-Naeini, *Feedback Control of Dynamic Systems*. Prentice-Hall, Upper Saddle River, New Jersey, Fourth edition, 2002.
[2] N.S. Nise, *Control Systems Engineering*. Wiley, Hoboken, New Jersey, Fourth edition, 2008.
[3] A. Packard, G. Balas, M. Safonov, R. Chiang, P. Gahinet, A. Nemirovski, *Robust Control Toolbox*, The Mathworks [On line]. Available at http://www.mathworks.com/access/helpdesk/help/toolbox/robust/.
[4] W. Messner, M. Bedillion, L. Xia, and D. Karns, "Lead and lag compensators with complex poles and zeros: design formulas for modeling and loop shaping," *IEEE Control Systems Magazine*, vol. 27, no. 1, Feb 2007, pp. 44-54.
[5] W. Messner, "Some advances in loop shaping with applications to disk drives," *IEEE Transactions on Magnetics*, vol. 37, no. 2, Mar 2001, pp. 651-656.
[6] L. Xia and W. Messner, Loop Shaping for Robust Performance Using the RBode plot. *Proceedings of the 2005 American Controls Conference*, Portland, OR, June 2005, p. 2869-74.
[7] L. Xia and W. Messner, An Improved RBode Plot. *Proceedings of the 2008 American Controls Conference*, Seattle, WA, June 2008.
[8] J. Doyle, B. Francis and A. Tannenbaum, *Feedback Control Theory*. Macmillan Publishing Company, 1992.
[9] W. Messner, Clasical Control Revisited: Variations on a Theme. *Proceedings of the 2008 Workshop on Advanced Motion Control*, Trento, Italy, March 2008.